Outer-Sphere Investigation of MRI Relaxation Contrast Agents. Example of a Cyclodecapeptide Gadolinium Complex with Second-Sphere Water

Célia S. Bonnet,[†,§] Pascal H. Fries,*[,†] Serge Crouzy,[‡] and Pascale Delangle*[,†]

CEA, INAC, Service de Chimie Inorganique et Biologique (UMR_E 3 CEA UJF, FRE 3200 CNRS), 38054 Grenoble, France and CEA, iRTSV, Laboratoire Chimie et Biologie des Métaux (UMR 5249 CEA CNRS UJF), F-38054 Grenoble, France

Received: February 16, 2010; Revised Manuscript Received: April 28, 2010

We show how the purely outer-sphere (OS) relaxivity of a probe solute due to a Gd^{3+} complex can help characterize the outer (O), inner (I), and second (2) sphere (S) contributions to the water proton relaxivity. Because of the difficulties of accurate theoretical predictions, we propose an experimental determination of the OS dipolar time correlation function (OS-DTCF) of the relative position of Gd^{3+} with respect to any of the equivalent protons of the purely OS probe p-dioxane, which moves around the complex without binding to it. The method is illustrated by the GdPA complex with PA = c(AspArgGluProGlyGluTrpAspProGly). The experimental DTCF for dioxane is obtained by a model-free analysis of the high-field relaxivity of its protons. The time-modulation of the dioxane DTCF by the Gd^{3+} electronic spin relaxation yields a measurable quenching of the longitudinal relaxivity at low-to-medium field, which serves us to deduce the fluctuating zero-field splitting (ZFS) Hamiltonian causing this electronic relaxation. The DTCF for water is derived from that for dioxane by appropriate scaling of the geometry of collision and relative diffusion coefficients of these molecules with respect to GdPA. The information obtained on the OS motion for water and the ZFS Hamiltonian together with an independent characterization of the IS contribution allows us to disentangle the OS, IS, and 2S mechanisms and interpret the relaxivity profile of the water protons from 2.35 mT to 18.8 T. The presence of a large 2S contribution is confirmed.

1. Introduction

The Gd^{3+} ion has the highest possible value $S = 7/2$ of total electronic spin due to its seven unpaired 4f electrons and thus an exceptionally large paramagnetic moment $\gamma_S \hbar \mathbf{S}$, where γ_S is approximately the gyromagnetic ratio of the spin of an electron.[1] When Gd^{3+} complexes GdL (L = ligand) are dissolved in a liquid placed in an applied magnetic field $\mathbf{B}_0$, the Gd^{3+} moments considerably accelerate the longitudinal relaxation rates $R_1 \equiv 1/T_1$, transverse relaxation rates $R_2 \equiv 1/T_2$, and longitudinal relaxation rates in the rotating frame[2] $R_{1\rho} \equiv 1/T_{1\rho}$ of the nuclear spins I on the various solvent and solute molecules M_I in the solution.[3−7] The longitudinal relaxivity r_1, transverse relaxivity r_2, and longitudinal relaxivity in the rotating frame $r_{1\rho}$ of a nuclear spin are respectively defined as the paramagnetic enhancements of its relaxation rates R_1, R_2, and $R_{1\rho}$ per millimolar of dissolved complex[8−11] (see Supporting Information, Subsection I.1). In magnetic resonance imaging (MRI), the relaxivity r_1 of the water proton (spin) is of particular importance since it gives the efficiency of the Gd^{3+} complex to improve the contrast of T_1-weighted magnetic resonance images.[9] Relaxivities vary with the properties of the complex, named contrast agent (CA), and the value of the imaging field $\mathbf{B}_0$. The chemistry of CAs is a very active field of research.[12−16] Its goal is to optimize the structure and dynamics of the complexes to attain the maximal relaxivity of the water proton at a given field. For that purpose, the relaxivities are expressed in terms of molecular parameters that can be tailored by the chemist. The relaxivities depend on the random relative motion of I with respect to S. For a hydrogen proton of a water molecule, they are generally ascribed to three types of intermolecular dynamics of the water molecule with respect to the complex.[8−11] These dynamics are (i) the outer-sphere (OS) dynamics that corresponds to the relative translational and rotational Brownian motions of a free water molecule with respect to GdL, (ii) the inner-sphere (IS) dynamics where the water molecule coordinated to Gd^{3+} follows the complex in its Brownian reorientation and exchanges with the surrounding free water molecules, and (iii) the second-sphere (2S) dynamics where the water molecule significantly binds to functional groups of the ligand L, also rotates with the complex, and exchanges with the surrounding free water molecules. This description already involves many adjustable parameters so that refinements such as the possible direct exchange between the IS and 2S water molecules are neglected. The measured relaxivities are the sums of the OS, IS, and 2S contributions stemming from these spatial dynamics

$$r_\alpha = r_\alpha^{OS} + r_\alpha^{IS} + r_\alpha^{2S} \quad (\alpha = 1, 2, 1\rho) \tag{1}$$

In general, they depend not only on the interspin spatial motion, but also on the relaxation dynamics (fluctuating quantum dynamics) of the Gd^{3+} electronic spin. Indeed, their theoretical expressions are linear combinations (of real parts) of Fourier transforms of quantum time correlation functions (TCFs) of the components of the dipolar local field[17−19] $\mathbf{B}_S$ created by the magnetic moment $\gamma_S \hbar \mathbf{S}$ of the electronic spin S at the position

* To whom correspondence should be addressed. (P.H.F.) Tel.: +33438783107. Fax: +33438785090. E-mail: pascal-h.fries@cea.fr. (P.D.) Tel.: +33438789822. Fax: +33438785090. E-mail: pascale.delangle@cea.fr.
† INAC.
‡ iRTSV.
§ Present address: Centre de Biophysique Moléculaire, CNRS, Rue Charles Sadron, 45071 Orléans Cedex 2, France.

10.1021/jp101443v
Published on Web 06/16/2010

of the nuclear spin I. Their description in terms of models of spatial motion and electronic spin dynamics, both tractable and accurate, is an experimental and theoretical challenge taken up progressively.[6−11] In the race toward efficient contrast agents, it was early recognized that the IS relaxivity considerably increases at typical moderate imaging fields $B_0 \cong 1$ T for complexes of long rotational correlation time τ_r, that is, of high molecular weight.[20] This property already stems from the simplest picture of IS spatial motion, that is, an isotropic rotational diffusion of the complex, which turns out to be reasonably accurate because the effects of the diffusion anisotropy of the complex on the intramolecular nuclear relaxation are rather small unless the shape of the complex is an unusually very flat disk or elongated rod,[21] especially in the extreme narrowing regime.[22] In contrast, bringing to light the origin of electronic spin relaxation has been problematic.[8,23,24] In the generally admitted description, electronic spin relaxation was only due to a fast fluctuating transient zero field splitting (ZFS) Hamiltonian originating from the fast local intramolecular motions ("vibrations") of the Gd^{3+} coordinating atoms. This model implied a possible relaxivity quenching at $B_0 \cong 1$ T for chelates of low and moderate molecular weights. This concern was ruled out when it was shown that multiple frequency and temperature EPR data of complexed Gd^{3+} ions[23,24] can be satisfactorily interpreted by introducing an additional natural ZFS Hamiltonian that is static in a molecular frame rigidly bound to the complex.[25−27] Indeed, the observed fast decay of the longitudinal electronic spin relaxation at low field, which dramatically quenches the relaxivity, can be then correctly attributed to the fluctuations of the static ZFS Hamiltonian caused by the Brownian rotation of the complex.[17] These fluctuations are slow enough to ensure a rapid dispersion (decrease) with field of the longitudinal electronic spin relaxation rate[28−30] $1/T_{1e}$, which becomes smaller than the rates of the spatial fluctuations of the OS, IS, and 2S mechanisms, so that electronic spin relaxation hardly affects relaxivity above 1 T.[11] However, optimizing the electronic relaxation time T_{1e} is still a challenge[31,32] when developing large Gd^{3+} CAs with $\tau_r > 1$ ns for high IS relaxivity.[12,14,16,33,34] Indeed, at $B_0 \cong 1$ T, T_{1e} is governed by the fluctuations of the transient ZFS Hamiltonian and in the range 1−10 ns, so that it can determine the effective correlation time τ_{c1}, defined as $1/\tau_{c1} \equiv 1/\tau_r + 1/T_{1e}$, of the intramolecular relaxation rate $1/T_{1M}$ of the IS mechanism.[19] Furthermore, the evaluation and description of the OS and 2S mechanisms should be significantly improved in view of their important potential contributions to relaxivity.[4,10,16,35−39] For instance, though the OS dynamics accounts for about one-half of the relaxivity of commercial CAs such as Gd(dtpa) (dtpa = diethylene triamine pentaacetate),[4] it is almost always described by the Ayant, Belorizky, Hwang, and Freed[40,41] (ABHF) model, where the Gd^{3+} ion and the water proton are assumed to be at the centers of hard spheres that have a collision diameter a_{GdH} corresponding to an effective Gd^{3+}−proton minimal distance of approach and undergo a relative motion described by the usual diffusion equation. This picture is oversimplified since the water proton I has a much more complicated relative motion with respect to the Gd^{3+} electronic spin S, induced by the anisotropic free translational and rotational Brownian motions of the colliding water molecule and Gd^{3+} complex and due to the anisotropic shapes and charge distributions of these species. Our understanding of the 2S mechanism is even more vague despite a promising contribution to relaxivity for various ligands bearing H-bonding atoms.[10] In the simplest possible description, the number of 2S water molecules, the distances of their protons to Gd^{3+}, and their residence times are merely adjustable parameters with few physical restraints.

This paper deals with three open issues of relaxivity, that is, the characterization of (i) the electronic spin relaxation that can control the efficacy of macromolecular CAs, (ii) the OS contribution, and (iii) the 2S contribution. The method is based on the determination of the OS-DTCF of a (purely) OS probe,[42] that is, a diamagnetic species carrying a proton spin and having a purely OS dynamics with respect to the complex. We show how the fluctuating ZFS Hamiltonian responsible for the Gd^{3+} electronic spin relaxation can be determined from the quenching of the longitudinal relaxivity of the probe proton at low and medium field. This procedure only needs commercial NMR instruments (see Supporting Information, Subsection I.1) and gives the information on electronic spin relaxation, which is required for the relaxivity analysis and generally derived from comprehensive EPR studies.[23,24,27,32,43,44] We infer the OS-DTCF for water from that of the probe and derive the water proton relaxivity r_α^{OS}. Once we have obtained reliable values of the IS and OS relaxivities, the 2S contribution is derived unambiguously as the residual $r_\alpha^{2S} \equiv r_\alpha^{exp} - r_\alpha^{OS} - r_\alpha^{IS}$, where r_α^{exp} is the experimental relaxivity.

The example chosen to illustrate these methods is the recently prepared complex of Gd^{3+} with the cyclodecapeptide c(AspArgGluProGlyGluTrpAspProGly) (PA) that incorporates two prolylglycine sequences as β-turn inducers and carries four side chains with acidic carboxyl groups for lanthanide Ln^{3+} complexation.[39] The conformation of the GdPA complex is shown in Figure 1.

At high field, the IS contributions to r_α were calculated from molecular parameters derived from a cross-analysis of independent experimental informations. The theoretical OS relaxivities were estimated from the hard-sphere ABHF model with reasonable parameters. The IS + OS contributions $r_\alpha^{IS} + r_\alpha^{OS}$ were 30% lower than the experimental values (see ref 39, Figure 5). This led us to propose a large 2S contribution to relaxivity due to the interaction of water molecules with the hydrophilic peptide ligand via hydrogen-bonding. A major goal of this work is to confirm this important 2S mechanism by using an accurate description of the OS dynamics yielding more reliable OS relaxivities. We will also interpret the longitudinal proton relaxivities of a probe solute and water in the low-to-medium field domain to get a complete picture of the molecular mechanisms governing relaxivity.

The paper is organized as follows. In Section 2 we recall the expressions of the relaxivities r_α^{OS}, r_α^{IS}, and r_α^{2S} used by the Grenoble method[17,19] in the high and low-to-medium field domains. In particular, we give the OS contributions r_α^{OS} in terms of the OS-DTCF $g_2(t)$. In Section 3, we simulate the OS geometry of collision and the presence of 2S water with the help of elementary force fields and standard classical molecular dynamics. In Section 4, we retain p-dioxane $C_4H_8O_2$ as a convenient OS probe for GdPA and derive the OS-DTCF $g_2(t)$ of its protons from their "star" relaxivity[42] r_*^{OS} measured at high-field in D_2O. The fluctuating ZFS Hamiltonian is obtained in Section 5 by the quenching of the longitudinal relaxivity of the probe proton at low-to-medium field. In Section 6, we propose an approximate expression of $g_2(t)$ for the HOD proton in terms of its counterpart for the probe protons. We interpret the relaxivity of the water protons due to GdPA versus magnetic field, also named nuclear magnetic relaxation dispersion (NMRD), in terms of the OS, IS, and 2S contributions.

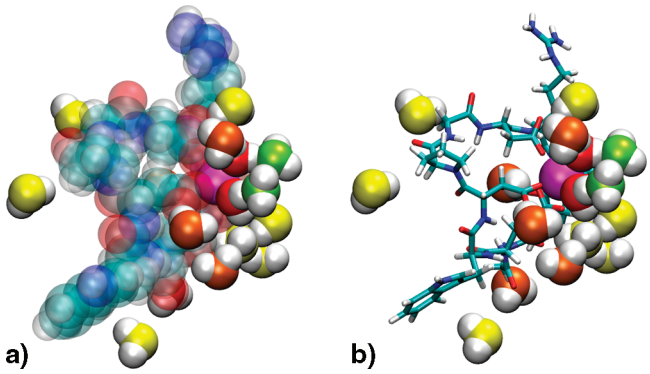

Figure 1. Simulated possible conformation of the GdPA complex in water. The Gd^{3+} ion (magenta) is surrounded by IS water (red oxygen), 2S water (orange oxygen), and OS water (yellow or green oxygen). The defining criterion for a 2S water molecule is to be different from prescribed IS water and to stay near Gd^{3+} for a sufficiently long time given by a MD simulation. The existence of OS water molecules (green oxygen) in contact with IS water demonstrates the possibility of direct exchange between IS and OS water without necessary step in the middle of 2S water as for the aqua metal cations. (a) The van der Waals representation of the atoms displays the volumes of GdPA and water. (b) The licorice openwork representation of the ligand PA gives a clearer and more complete picture of IS and 2S water around Gd^{3+}. It is the starting snapshot of the simulated possible relative motions of the water molecules with respect to Gd^{3+} which can be viewed for a 100 ps duration by playing the .mpeg video file in Supporting Information. This Supporting Information movie shows the large amplitudes of the displacements of the OS water molecules with respect to GdPA despite the artificial periodic boundary conditions of the simulation box. These amplitudes are displayed in angstroms for the OS water molecules with green oxygen. The residence times of the 2S water molecules near GdPA are significant and even exceed the duration of the displayed dynamics as exemplified by the 2S water molecule initially behind the ligand with respect to Gd^{3+}. During this short simulation, the IS water molecules remain bound to Gd^{3+}, but librate with respect to this ion.

2. Relaxivities

Let $g_S \cong 2$ be the Landé factor of the electronic spin S. The relaxivities depend on the gyromagnetic ratios γ_I and $\gamma_S \equiv -g_S\mu_B/\hbar$ of the interacting spins I and S through the dipolar coupling factor $A \equiv (8\pi/5)\gamma_I^2\mu_{eff}^2$, where μ_{eff} is the Gd^{3+} effective electronic magnetic moment given by $\mu_{eff} \equiv g_S\mu_B[S(S+1)]^{1/2}$. They also depend on the field B_0, in particular through the angular Larmor frequencies $\omega_I = 2\pi\nu_I \equiv -\gamma_I B_0$, $\omega_S \equiv -\gamma_S B_0$ of the spins. They are complicated functions of the intermolecular spatial motion of M_I with respect to the complex and of the quantum relaxation dynamics of S as discussed hereafter. We successively consider the OS, IS, and 2S relaxivities in the high and low-to-medium field regimes.

2.1. High-Field Regime. In the high-field domain $B_0 \geq 3$ T, within the Redfield limit[5,6] and even beyond[17,30] the relaxivities are independent of the electronic spin relaxation because the terms involving the transverse electronic relaxation become negligible while the remaining terms are no longer affected by the longitudinal electronic relaxation because its decay rate, roughly in B_0^{-2}, becomes much lower than those of the IS and OS DTCFs.

2.1.1. High-Field Outer-Sphere Relaxivity. The theory of OS relaxivity rests on the OS dipolar time correlation function (DTCF) $g_2(t)$, a suitable expression of which is given in eq 2. Equivalent formulations of this general intermolecular relaxation property can be used.[22,40,41] In the laboratory (L) frame, let (r,θ,ϕ) be the spherical coordinates of the interspin vector $\mathbf{r}$. Let $Y_{2q}(\theta,\phi)$ $(-2 \leq q \leq 2)$ be the spherical harmonics of order 2. The OS-DTCF $g_2(t)$ of the random function $r^{-3}Y_{2q}(\theta,\phi)$ is independent of the index q and defined as[45]

$$g_2(t) = 10^{-6}N_A \int\int \frac{Y_{2q}(\theta_0,\phi_0)}{r_0^3}\frac{Y_{2q}^*(\theta,\phi)}{r^3} g^{OS}_{\text{site } I\text{-site } S}(r_0)\rho(\mathbf{r}_0,\mathbf{r},t)\mathrm{d}\mathbf{r}_0\,\mathrm{d}\mathbf{r} \quad (2)$$

where $g^{OS}_{\text{site } I-\text{site } S}(r_0)$ is the pair distribution function of the interspin distance and $\rho(\mathbf{r}_0,\mathbf{r},t)$ is the OS propagator describing the random evolution of the interspin vector $\mathbf{r}$ in the course of time. More precisely, $\rho(\mathbf{r}_0,\mathbf{r},t)$ is the probability that the interspin position is $\mathbf{r} \equiv (r,\theta,\phi)$ at time t given that it was $\mathbf{r}_0 \equiv (r_0,\theta_0,\phi_0)$ at initial time $t = 0$. It results from the anisotropic translational and rotational Brownian motions of M_I and GdL without binding. A key property of the OS dynamics is the translational correlation time τ which characterizes the time decay of $g_2(t)$ and is defined as follows. Introduce the collision diameter b of M_I and GdL, which is loosely defined when these molecules are soft and/or anisotropic. Consider the relative diffusion coefficient $D_{M_I\text{-GdL}}$ of M_I and GdL, hereafter denoted by D, which is the sum $D = D^t_{M_I} + D^t_{GdL}$ of the self-diffusion coefficients of these species. The translational correlation time is

$$\tau \equiv b^2/D \quad (3)$$

The OS relaxivities are linear combinations of the "ideal" usual spectral density $j_2(\omega)$ of $g_2(t)$ defined as[42]

$$j_2(\omega) = \int_0^\infty g_2(t)\cos(\omega t)\mathrm{d}t \quad (4)$$

They have the simple forms[39,42,45] $(r_{1\rho}^{OS,\text{ high-field}} = r_2^{OS,\text{ high-field}})$

$$r_1^{OS,\text{ high-field}} = Aj_2(\omega_I)$$
$$r_2^{OS,\text{ high-field}} = A\left[\frac{2}{3}j_2(0) + \frac{1}{2}j_2(\omega_I)\right] \quad (5)$$

2.1.2. High-Field Inner- and Second-Sphere Relaxivities. The usual models are briefly recalled now for water. The IS relaxivities are reasonably evaluated as follows. They depend on the structure of the complex[8−11] since they are proportional to the number q of coordinated water molecules carrying the IS protons H and decrease rapidly with the mean Gd- H distance r_H as $1/r_H^6$. They are functions of the rotational Brownian dynamics of the complex assumed to be isotropic and characterized by a single rotational correlation time τ_r. They depend on the mean residence time τ_M of a coordinated water molecule. Let $P \equiv 10^{-3}$ M/55.5 M $= 1.8 \times 10^{-5}$ be the ratio of the numbers of complexes and water molecules in a 1 mM solution of GdPA complexes. The high-field IS relaxivities have the simple Luz and Meiboom forms[8−11]

$$r_\alpha^{IS} = Pq/(T_{\alpha M} + \tau_M) \quad (6)$$

where $T_{\alpha M}$ are the intramolecular (intracomplex) relaxation times of the protons of hypothetic permanently coordinated water molecules. The associated relaxation rates $R_{\alpha M} \equiv 1/T_{\alpha M}$ $(R_{1\rho M} = R_{2M})$ are given by[19]

$$\frac{1}{T_{1M}^{\text{high-field}}} = A\frac{1}{4\pi r_H^6}\frac{\tau_r}{1+\omega_I^2\tau_r^2}$$
$$\frac{1}{T_{2M}^{\text{high-field}}} = A\frac{\tau_r}{4\pi r_H^6}\left[\frac{2}{3}+\frac{1}{2}\frac{1}{1+\omega_I^2\tau_r^2}\right] \quad (7)$$

Since the present simple IS theory is sufficient to account for all the experimental data, we do not resort to more elaborate descriptions involving, for instance, the possible internal motion of IS water and additional adjustable parameters.[34,46]

To within a rough approximation, the 2S relaxivities depend on the ligand solvation structure in a way similar to their IS counterparts.[9,10] They are proportional to the number q' of the so-called 2S water molecules which are noncovalently bound to the ligand and carry the 2S protons H. They decrease with the mean Gd−H distance r'_H of these protons as $1/(r'_H)$.[6] They are also functions of the rotational correlation time τ_r and of the mean residence time τ'_M of a 2S water molecule. The expressions of r_α^{2S} are similar to those of r_α^{IS} and given by eqs A1 to A3 in Supporting Information Appendix A.

Four independent parameters (q, r_H, τ_r, τ_M) define the standard model of IS motion just recalled. Three additional independent parameters q', r'_H, τ'_M besides τ_r determine the simplified model of 2S dynamics given by (q', r'_H, τ_r,τ'_M). The simplest picture of OS motion, the hard-sphere ABHF model, depends on two additional parameters, the collision diameter a_{GdH} corresponding to an effective Gd^{3+} - proton minimal distance of approach and the relative diffusion coefficient D_w of water with respect to the complex. As discussed previously,[39] at most five of these nine independent parameters, i.e., (q, r_H, τ_r, τ_M) that characterize the IS dynamics and D_w, can be measured by experimental techniques other than water proton relaxivity. Only little additional information on the OS and 2S processes can be derived from auxiliary measurements of the sole water proton relaxivity at low-to-medium field since its interpretation is confused by the effects of electronic spin relaxation. Using an OS probe helps to disentangle these effects from those due to OS and 2S motions and yields a reliable picture of the molecular processes at the origin of relaxivity.

2.2. Electronic Spin Relaxation. The theoretical relaxivities r_α^{OS}, r_α^{IS}, and r_α^{2S} are linear combinations (of real parts) of Fourier transforms of quantum time correlation functions (TCFs) of the fluctuating components of the dipolar local field[17,19] $\mathbf{B}_S$ created by the magnetic moment $\gamma_S\hbar\mathbf{S}$ of the electronic spin S at the position of the nuclear spin I. The components of $\mathbf{B}_S$ depend on the interspin $I-S$ vector $\mathbf{r}(t)$ and on the component operators $S_d(t)$ ($S_d = S_+, S_-, S_z$, d = direction) of $\mathbf{S}$ (see Supporting Information Appendix A in ref 19). The Brownian rotation and vibrations of the complex produces a random modulation of the ZFS Hamiltonian $H_{ZFS}^{(L)}(t)$ in the laboratory (L) frame. This modulation induces time fluctuations of the quantum states of the spin S at the origin of the fluctuations or equivalently relaxation of the spin operator values.[6,17,19,30,47] The ZFS Hamiltonian is due to the ligand field via second-order perturbation effects of the spin−orbit coupling of the Gd^{3+} 4f electrons. To evidence the two time-scales of the fluctuations of the ZFS Hamiltonian, it is convenient to express this Hamiltonian in a molecular (M) frame rigidly bound to the complex. In the (M) frame, the ZFS Hamiltonian $H_{ZFS}^{(M)}(t)$ has a "vibration" (v) -averaged value $H_{ZFS,S}^{(M)}$ which is static (S), that is, independent of time by construction. It is generally sufficient to approximate $H_{ZFS,S}^{(M)}$ by its second-order terms in the electronic spin components, so that it can be characterized by the two ZFS intensity parameters D_S and E_S. The magnitude of $H_{ZFS,S}^{(M)}$ is $\Delta_S \equiv (2D_S^2/3 + 2E_S^2)^{1/2}$ and its characteristic fluctuation time in the (L) frame is the rotational correlation time τ_r of the complex. The transient (T) ZFS Hamiltonian is simply the difference $H_{ZFS,T}^{(M)}(t) \equiv H_{ZFS}^{(M)}(t) - H_{ZFS,S}^{(M)}$. The simplest model of fluctuating transient ZFS Hamiltonian is the Brownian pseudorotation of $H_{ZFS,T}^{(M)}(t)$, again restricted to its second-order terms in the electronic spin components. Its effects on the electronic spin relaxation are given by its magnitude Δ_T and a loosely called vibrational correlation time τ_v. Here, the concept of vibrations, which modulate $H_{ZFS}^{(M)}(t)$, accounts for damped vibrations, but also for possible small conformational changes of the ligand such as those shown in Figure 1A of ref 39 and the .mpeg video file described in Figure 1, so that τ_v is expected to have an effective value of the order of a few picoseconds, much shorter than τ_r. Here, we assume the simplest situation, $E_S = 0$, so that the fluctuations of the ZFS Hamiltonian are governed only by the four parameters D_S, τ_r, Δ_T, τ_v. Then, three additional independent parameters D_S, Δ_T, τ_v have to be determined to interpret the relaxivity values at low-to-medium field.

In this work, following common practice,[44,48−50] the static and transient ZFS Hamiltonians are simply approximated by their second rank terms $H_{ZFS,S,2}^{(L)}(t)$ and $H_{ZFS,T,2}^{(L)}(t)$, despite possible contributions of the fourth and particularly sixth order terms $H_{ZFS,S,4}^{(L)}(t)$ and $H_{ZFS,S,6}^{(L)}(t)$ of the static ZFS Hamiltonian.[27,28,51] Indeed, even in the tractable Redfield limit,[5,6] the effects of the ZFS Hamiltonians $H_{ZFS,S,k}^{(L)}(t)$ ($k = 2, 4, 6$) give rise to contributions to the Gd^{3+} electronic spin relaxation, the theoretical expressions of which involve many spectral densities of the rotational time correlation functions of these Hamiltonians with characteristic times $\tau_r^{(k)} = 6\tau_r/(k(k+1))$, that is, $\tau_r^{(2)} = \tau_r$, $\tau_r^{(4)} = 0.3\tau_r$, and $\tau_r^{(6)} = \tau_r/7$.[27,28,51] Detailed experimental information on the electronic relaxation, for instance, EPR spectra at multiple frequencies and temperatures, is necessary to disentangle the contributions of these partial Hamiltonians and obtain their magnitudes. Here, the information derived from the relaxivity quenching is sufficient to derive static and transient ZFS Hamiltonians of order 2 characterized by very different correlation times τ_r and τ_v. We will see that this simple picture is supported by its very satisfactory predictions. A more refined analysis of the static ZFS Hamiltonian would require independent complementary experimental studies.

2.3. Low-to-Medium-Field Regime. In the field domain $B_0 < 3$ T, the relaxivity quenching by the electronic spin relaxation can rise dramatically with decreasing field.[3−7,17,19]

2.3.1. Outer-Sphere Relaxivity. The time fluctuations of the random spatial function $r^{-3}Y_{2q}(\theta,\phi)$ of the interspin vector are mainly governed by the OS relative translational diffusion of the OS probe with respect to the GdPA complex, whereas the time fluctuations of the quantum states of the spin S stem from the Brownian rotation and vibrations of the complex. The random dynamics of the spatial interspin variables and of the electronic spin states are uncorrelated[6,47,52,53] in the expression of the dipolar local field[17,19] $\mathbf{B}_S$ at the origin of the relaxivity. Then, the effects of the electronic spin relaxation on the OS relaxivity are simply taken into account by the so-called longitudinal and transverse TCFs $G_{//}^{nor}(t,B_0)$ and $G_{\perp}^{nor}(t,B_0)$ of the electronic spin components[30,45] $S_z//\mathbf{B}_0$ and $S_- \equiv S_x - iS_y \perp \mathbf{B}_0$ (decomposition approximation[6,47,52,53]). More precisely, introducing the longitudinal and transverse spectral densities

$$j_{2//}(\omega_I,B_0) = \int_0^\infty g_2(t)G_{//}^{nor}(t,B_0)\cos(\omega_I t)\mathrm{d}t$$
$$j_{2\perp}(\omega_S) = \mathrm{Re}\int_0^\infty g_2(t)G_{\perp}^{nor}(t,B_0)\mathrm{d}t \quad (8)$$

with $B_0 = -\omega_I/\gamma_I = -\omega_S/\gamma_S$, the longitudinal relaxivity r_1^{OS} is given by eq 9.

$$r_1^{OS} = Aj_{2//}(\omega_I, B_0) + \frac{7}{3}Aj_{2\perp}(\omega_S)$$
$$= A\int_0^\infty g_2(t)G_{//}^{nor}(t, B_0)\cos(\omega_I t)\mathrm{d}t + \frac{7}{3}A\mathrm{Re}\int_0^\infty g_2(t)G_\perp^{nor}(t, B_0)\mathrm{d}t \quad (9)$$

In the ideal situation of an infinitely slow electronic spin relaxation, the electronic TCFs simplify to $G_{//}^{nor} = 1$ and $G_\perp^{nor} = \exp(i\omega_S t)$, so that r_1^{OS} takes its ideal form

$$r_1^{OS,id} = Aj_2(\omega_I) + \frac{7}{3}Aj_2(\omega_S)$$
$$= A\int_0^\infty g_2(t)\cos(\omega_I t)\mathrm{d}t + \frac{7}{3}A\int_0^\infty g_2(t)\cos(\omega_S t)\mathrm{d}t \quad (10)$$

which is the weighted sum of the cosine Fourier transforms of $g_2(t)$ calculated at the nuclear and electronic Larmor frequencies ω_I and ω_S.

2.3.2. Inner- and Second-Sphere Relaxivities. As shown above, the decomposition approximation holds for the OS relaxivity and leads to a simple treatment of the effects of the electronic spin relaxation in terms of the electronic TCFs. In contrast, the decomposition approximation fails for the IS (and 2S) relaxation mechanisms[6,17,19,47,52] and the orientations $\hat{u}(\overrightarrow{GdH_p})$ in the (M) frame of the vectors $\overrightarrow{GdH_p}$ joining Gd^{3+} to the protons H_p of the various IS and 2S water molecules enter any exact calculation of the corresponding relaxivities. Unfortunately, the experimental determination of the three additional angular parameters defining the positions of the two protons of an IS or 2S water molecule is not feasible. Therefore, it is assumed that the longitudinal IS relaxivity r_1^{IS} is still given by eq 6, in which our ignorance about the orientations $\hat{u}(\overrightarrow{GdH_p})$ leads to replace T_{1M} by $\bar{T}_{1M}$, where the rate $1/\bar{T}_{1M}$ is the weighted sum[19]

$$\frac{1}{\bar{T}_{1M}} = w_{\hat{x}_S}\frac{1}{T_{1M}(\hat{x}_S)} + w_{\hat{y}_S}\frac{1}{T_{1M}(\hat{y}_S)} + w_{\hat{z}_S}\frac{1}{T_{1M}(\hat{z}_S)} \quad (11)$$

In eq 11, $1/T_{1M}(\hat{x}_S)$ (respectively $1/T_{1M}(\hat{y}_S)$, $1/T_{1M}(\hat{z}_S)$) is the relaxation rate of the IS water proton H_p such that $\overrightarrow{GdH_p}$ is parallel to the principal direction $\hat{x}_S$ (respectively $\hat{y}_S$, $\hat{z}_S$) of the static ZFS Hamiltonian of order 2 in a GdL molecular (M) frame. The relaxation rate $1/T_{1M}(\hat{u})$ ($\hat{u} = \hat{x}_S, \hat{y}_S, \hat{z}_S$) is obtained by computing eq 4 of ref 17 according to the Grenoble method in which the rotation and vibrations of the complex are simulated by random walks. The weight $w_{\hat{u}} \geq 0$ is associated with the relaxation rate $1/T_{1M}(\hat{u})$. The weights satisfy the equality $w_{\hat{x}_S} + w_{\hat{y}_S} + w_{\hat{z}_S} = 1$ and account for the different orientations of the vectors $\overrightarrow{GdH_p}$ of the various IS water protons. Because these orientations are generally unknown in the (M) frame, the weights can be assumed to be equal; $w_{\hat{x}_S} = w_{\hat{y}_S} = w_{\hat{z}_S} = 1/3$ in a first approximation.

The theory of the 2S relaxivities[9,10] mimics that of the IS relaxivities. The longitudinal 2S relaxivity r_1^{2S} is given by eqs A1, A4, and A5 of Supporting Information Appendix A.

3. Simulations and Molecular Models

The OS-DTCF $g_2(t)$ of a nuclear spin I coupled with an electronic spin S is simply given by eq 28 in ref 42 or eq E6 of the Supporting Information of this reference. However, its accurate computation by direct MD simulation or Brownian methods based on the molecular pair distribution function of the spin-carrying species is still a challenge.[42,54] This is particularly true when the paramagnetic species is a Gd^{3+} complex in solution, the accurate description of which requires heavy computations[55] to properly account for the many-body polarization interactions that are involved by such a highly charged ion and can represent up to 60% of the interaction energy.[56] We do not pursue in that direction since our goal is the determination of relaxivity properties from experiment within a simple, but reliable, parametrized theoretical framework, the molecular parameters of which can be optimized by chemistry. In this framework, the GdPA complex and the diamagnetic molecules X carrying the observed nuclear spins I are approximated as rigid species. The strong shape anisotropy of the complex derived from previous structural studies[39] is taken into account in the model used to calculate the OS relaxivity beyond current practice. When X is the water molecule, the strong electrostatic coordinating attraction of its negatively charged oxygen donor atom by Gd^{3+} and the H-bonding interactions of its hydrogen atoms with the oxygen and/or nitrogen atoms of PA give rise to IS and 2S bonds, respectively. To calculate the relaxivity properties, the complicated spatial motion of the formation and break of bonds is simply represented by finite bonding lifetimes, which nevertheless have to be derived from experiment and/or simulation. Here, the simulations are kept as simple as possible and only used to qualitatively determine the collision geometry in solution and indicate the presence of 2S water. Hereafter, we summarize the main results obtained on (i) the OS collision surface of a species X with the GdPA complex and (ii) the 2S water molecules possibly bound to the ligand. Technical details can be found in Supporting Information Section III.

3.1. Experimental Structure and Properties of Hydrated GdPA. The GdPA conformation shown in Figure 1 was determined from that of the apopeptide PA by combining CD spectroscopic information with proton NMR data and molecular mechanics simulations.[39] Luminescence titrations showed a reasonable stability of the LnPA complexes. The number $q = 2$ of metal-bound water molecules was obtained from the variation of the luminescence lifetimes of Tb^{3+} in the TbPA complex in H_2O/D_2O mixtures. Note that luminescence spectroscopy provides an accurate determination of the number q of IS water molecules since the 2S and OS water molecules, which are located at significantly larger distances from Tb^{3+}, have a very modest influence on the luminescence lifetime. The rotational correlation time $\tau_r = 386 \pm 15$ ps of the LnPA complexes was the result of converging determinations involving (i) the application of the Stokes−Einstein laws of rotational diffusion and self-diffusion where the self-diffusion coefficient of the analogous LaPA complex was measured by ^1H pulsed gradient spin echo (PGSE) NMR, (ii) the dipolar proton−proton longitudinal relaxation time of one of the glycine protons in the LaPA complex, and (iii) the high-field variation of the water proton relaxivities due to GdPA. Note that the applicability of the Stokes−Einstein diffusion laws supports the overall shape

and size of the complex. We assume that the distance of the IS water protons to the Gd^{3+} center has the most probable value[14,57] $r_H = 3.1$ Å. We could then propose a reliable model of the IS structure and dynamics characterized by the molecular parameters $r_H = 3.1$ Å, $q = 2$, $\tau_r = 386$ ps, and a coordination lifetime τ_M of the water molecule which is in the short-time category, that is, of the order of 10 ns,[58] but nevertheless much longer than τ_r, hence without effect on the relaxivity.

3.2. Gadolinium Force-Field and Coordination Restraints. All the MD simulations were performed with the CHARMM software.[59] The water molecules were described by the TIP3P model in which they are approximated as Lennard-Jones (LJ) spheres with three fixed embedded partial electric charges of constant values. We had to model the interaction of Gd^{3+} with water since no force field is available in CHARMM for this ion. We assumed that Gd^{3+} has its charge +3 of isolated ion and that water has the TIP3P charge distribution. Reasonable parameter sets of the LJ potential between Gd^{3+} and water oxygen were selected by prescribing that the associated simulation gives the experimental hydration free energy $\Delta G^0 = 818.4$ kcal/mol and the main experimental features of the Gd^{3+} first hydration sphere in the bulk, that is, about 8 coordinating water molecules and a Gd−water oxygen intercenter distance of approximately 2.4 Å. Among these parameter sets, we chose Sim2 of Supporting Information Table S5, for which the simulation best reproduces the coordination of Gd^{3+} by PA and two water molecules, which was proposed previously[39] and recalled in Subsection 3.1.

3.3. Outer-Sphere Collision Surface and Gadolinium Accessibility. The OS collision surface Σ_X of a solvent or solute molecule X with a complex GdL defines the accessibility of Gd^{3+} for X. This surface is a function of the molecular models used to represent GdL and X. The compact molecular packing in a liquid implies that the collisional configurations of two molecules are primarily determined by their very steep repulsive potential due to the Pauli exclusion principle of their electrons. Electrostatic and dispersion forces play important, but secondary roles. Therefore, the OS collision surface of X is simply made of the stop points of the bombardment trajectories of a large set of particles X directed toward the Gd^{3+} ion and stopped by the strong LJ repulsions of the atoms of the ligand PA and water molecules coordinating the ion. The simulated OS collision surfaces for p-dioxane and water are shown in Figure 2.

3.4. Second-Sphere Evidence. ***3.4.1. Structure.*** The Gd−O and Gd−H site−site distribution functions of the O and H atoms of water with respect of Gd^{3+} were computed for the force field Sim2 of Supporting Information Table S5. They are shown in Figure 3.

The second peaks of these functions were used to indicate the presence of possible 2S water molecules and their distances to Gd^{3+}.

3.4.2. Dynamics. A local accumulation of noncoordinating water molecules near Gd^{3+} revealed by the site−site distribution functions is insufficient to define a 2S region. The 2S water molecules should be also delayed in their translational Brownian motion by H-bonding attractions to the Gd^{3+} ligand.[60] Such a slowing down of the water molecules can be established by (i) computing the self-diffusion coefficient D_w^t of the water molecules in the bulk and (ii) showing that the residence times of the water molecules in the envisaged 2S region are significantly longer than those derived from the simulated value of D_w^t.

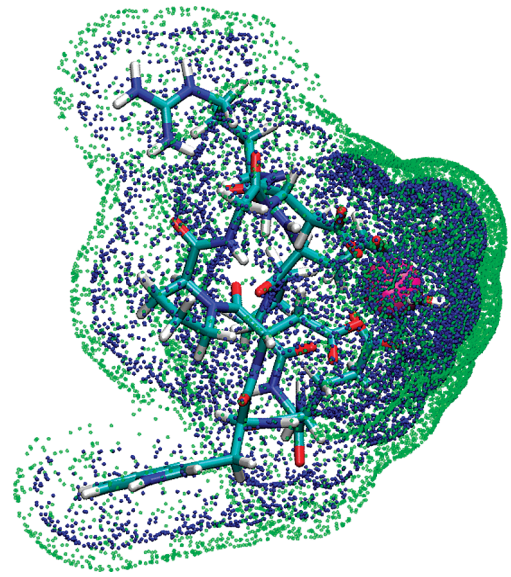

Figure 2. Superimposition of the OS collision surfaces Σ_X of X = water (blue points) and p-dioxane (green points). These surfaces define the accessibility of the complexed Gd^{3+} ion (magenta) for the OS molecules X and were obtained for a conformation of the GdPA complex with two IS water molecules derived by minimizing the energy of the complex and all the surrounding water molecules in the simulation box after thermal equilibration of the system.

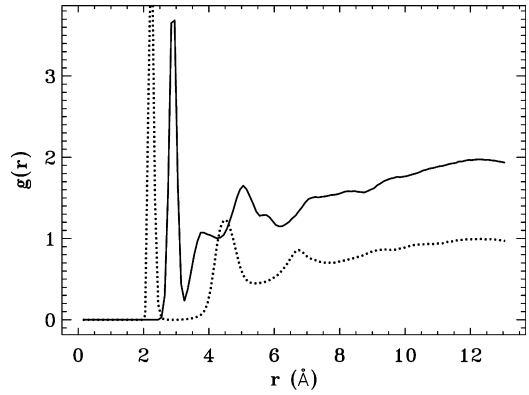

Figure 3. Pair distribution functions of the oxygen O (dotted curve) and hydrogen H (continuous curve) atoms of the water molecules with respect to Gd^{3+} for a model of GdPA in TIP3P water. Results derived from a MD simulation of 10 ns duration with 843 water molecules inside a 30 × 30 × 30 $Å^3$ periodic cubic box.

4. Outer-Sphere Intelligence Service to Decipher Relaxivity

As recalled in Section 3, it is difficult to describe the OS dynamics of a solvent or solute molecule M_I with respect to GdL and the associated DTCF $g_2(t)$. Here, for a purely OS probe, we show how this function can be derived from experimental data supplemented with model-free OS properties.

4.1. Choice of a Purely Outer-Sphere Probe. The general requirement for a solute M_I to be a purely OS probe is the absence of binding to the Gd^{3+} ion and ligand L.[45,61−64] Then, the probe should not contain coordinating groups. If the hydrogen atoms of water bond with L to produce 2S water as for the PA ligand, it should also be free of hydroxyl protons. Then, alcohols and molecules such as formaldehyde, which becomes a hydrate in water, are not suitable. In addition, the probe is expected here to have an OS dynamics that scales with that of water according to their relative diffusion coefficients with GdPA. Then, the probe should be electrically neutral as

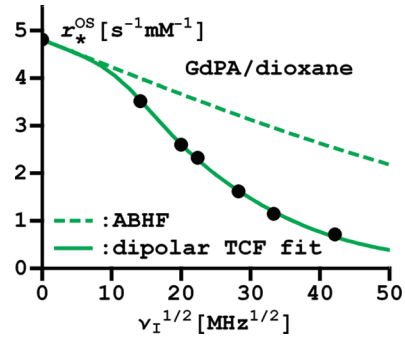

Figure 4. Field variation of the star relaxivity r_*^{OS} of the p-dioxane protons *I* due to GdPA in D_2O at 298 K. The dipolar TCF $g_2(t)$ of the OS relative dynamics of dioxane and GdPA was adjusted so as to yield a theoretical star relaxivity r_*^{OS} (continuous curve) reproducing the experimental values (dots). The ABHF model of r_*^{OS} (dashed curve) corresponds to the relative diffusion of hard spheres and is particularly defective: the large experimental zero-field value leads to a spin−spin collision diameter $a_{GdH} = 3.1$ Å, which is unrealistically small and incompatible with the large observed dispersion of r_{1*}^{OS} with field.

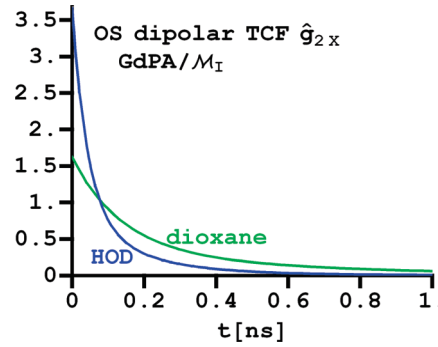

Figure 5. The "hat" dipolar TCFs $\hat{g}_2(t/\tau_0)$ governing the OS relaxivities of the p-dioxane and HOD protons due to GdPA in D_2O at 298 K.

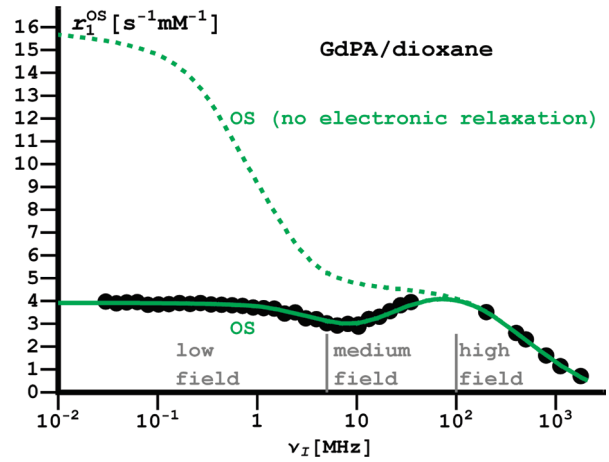

Figure 6. Longitudinal relaxivity profile of the p-dioxane protons *I* due to GdPA in D_2O at 298 K. The concentration of p-dioxane is ≅ 1 M.

water in order to have no charge−charge interactions with the locally charged groups of atoms of the complex since Coulomb interactions are known to significantly modify the OS dynamics.[65,66] The derivation of $g_2(t)$ for the probe rests on the measurement of its spectral density over the frequency range where it takes appreciable values. This requires a sufficiently slow self-diffusion of the probe, which nevertheless should keep a size not much larger than that of water in order to sense the same shape of the complex. Solutes such as dichloromethane CH_2Cl_2, acetone CH_3COCH_3, or p-dioxane $C_4H_8O_2$ are possible candidates. Para-dioxane was preferred because it has the highest number of equivalent protons and its concentration in water is not limited by a weak solubility as dichloromethane. Its self-diffusion, slightly slower than that of acetone, is also more favorable. Even at concentrations low enough to hardly affect the hydration of GdPA, the NMR signal of the p-dioxane protons is large so that accurate low-field relaxivity measurements are easy.

4.2. Dipolar Time Correlation Function of the Outer-Sphere Probe. It is convenient to introduce the "star" relaxivity[42] r_*^{OS} defined in eq 12

$$r_*^{OS} = Aj_2(\omega) = A\int_0^\infty g_2(t)\cos(\omega t)\mathrm{d}t \qquad (12)$$

This function is the Fourier transform of $g_2(t)$ up to the factor *A*, so that its knowledge over the whole frequency range yields $g_2(t)$ by inverse cosine Fourier transform. The challenge is to obtain the experimental values of r_*^{OS} over a frequency domain large enough to make possible this transform in an approximate, but nevertheless accurate way. This can be achieved[42] by using (i) the values of the relaxivities r_1^{OS} and $r_{1\rho}^{OS}$ measured at high field, (ii) the experimental relative translational diffusion coefficient *D* of the probe solute with respect to the Gd^{3+} complex and by noticing (iii) that the relaxivity $r_*^{OS} = r_1^{OS}$ at high field can be obtained at frequencies significantly higher than the frequencies of the available high-field spectrometers with the help of simple scaling laws for the temperature and field dependence. The experimental star relaxivity r_*^{OS} of the p-dioxane protons and its "inverse cosine Fourier transform" $g_2(t)$ given in the form of its hat expression[42] $\hat{g}_2(t/\tau_0)$ are shown in Figures 4 and 5, respectively.

5. Zero-Field Splitting Hamiltonian from Outer-Sphere Relaxivity

The measured longitudinal relaxivity r_1^{OS} of the p-dioxane protons is displayed in Figure 6.

At low and medium field, r_1^{OS} is much smaller than the ideal relaxivity $r_1^{OS,id}$ calculated by using the experimental dipolar OS-DTCF $g_2(t)$ displayed in Figure 5. Setting $\tau_r = 386$ ps, $E_S = 0$, the remaining ZFS Hamiltonian parameters $\Delta_S = (2/3)^{1/2}D_S = 0.04$ cm^{-1}, $\Delta_T = 0.024$ cm^{-1}, $\tau_v = 9$ ps (see Supporting Information IV.1) were obtained in two steps by fitting the theoretical values of r_1^{OS} given by eq 9 to their experimental counterparts at low and medium field. More precisely, the static and transient ZFS Hamiltonians are successively determined at low and medium field, where they respectively drive the electronic spin relaxation as explained in the comprehensive Figure 7. The electronic TCFs $G_{//}^{nor}$ and Re$[G_\perp^{nor}]$ caused by the fluctuating ZFS Hamiltonian of GdPA just derived can then be calculated at any field as described previously.[30,67] They are displayed in Figure 7a for field values that are typical of the three possible regimes of electronic spin relaxation.

Turn to the rationale of the success of the procedure employed to determine the ZFS Hamiltonian. The explanation depends only on the relative decay of $g_2(t)$ and is conveniently illustrated with its normalized (nor) form $g_2^{nor}(t) \equiv g_2(t)/g_2(0)$ shown in Figure 7 panel b or c.

In the low-field range, for example, $\nu_I = 1$ MHz, $G_{//}^{nor}$ and Re $[G_\perp^{nor}]$ have fast nonexponential time-decays of characteristic times of about 0.1 ns. Note that $G_\perp^{nor} \rightarrow G_{//}^{nor}$ at vanishing field because our 3D space is isotropic at zero field. If the ZFS Hamiltonian reduces to its sole transient part, $G_{//}^{nor}(t)$ has the

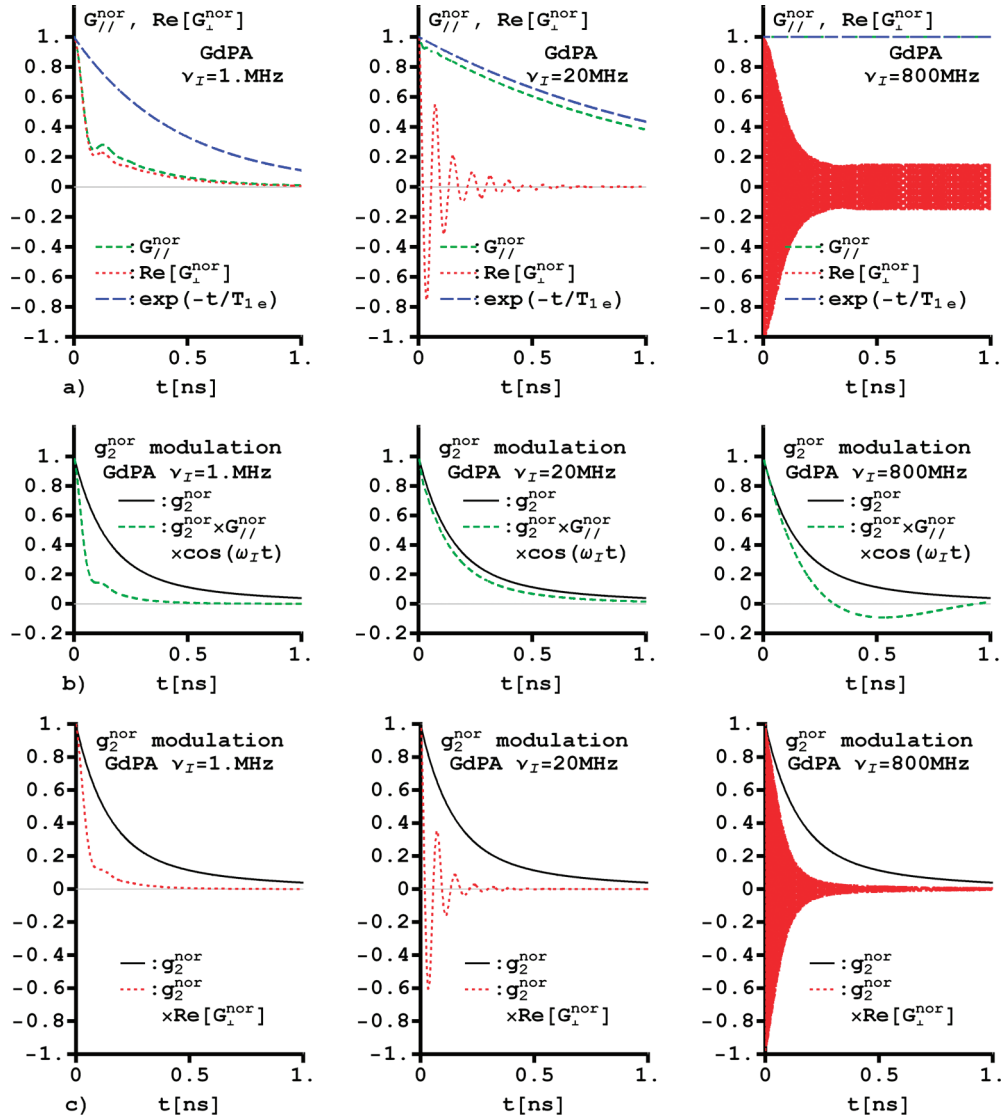

Figure 7. The normalized dipolar TCF $g_2^{nor}(t) \equiv g_2(t)/g_2(0)$ of the p-dioxane protons I due to the dioxane/GdPA relative motion in D_2O at 298 K and its modulation by the longitudinal and transverse TCFs $G_{//}^{nor}(t,B_0)$ and $G_{\perp}^{nor}(t,B_0)$ of the Gd^{3+} electronic spin in the low, medium, and high-field regimes (a) the electronic spin TCFs, (b) modulation by $G_{//}^{nor}(t,B_0)$, (c) modulation by $G_{\perp}^{nor}(t,B_0)$. The long-dashed curves in (a) represent the monoexponential decays of $G_{//}^{nor}(t,B_0)$ of characteristic relaxation times T_{1e} stemming from a purely transient ZFS Hamiltonian acting on the electronic spin.

monoexponential decay $G_{//T}^{nor} = \exp(-t/T_{1eT}^{McL})$, where the McLachlan (McL) longitudinal electronic relaxation rate is given by

$$\frac{1}{T_{1eT}^{McL}} \equiv \frac{1}{25}[4S(S+1) - 3]\Delta_T^2\tau_v\left[\frac{1}{1+\omega_S^2\tau_v^2} + \frac{4}{1+4\omega_S^2\tau_v^2}\right] \quad (13)$$

In the low-field range, the time-decay of $G_{//}^{nor}$, and thus of Re$[G_{\perp}^{nor}]$, is much faster than that of exp $(-t/T_{1eT}^{McL})$ due to the sole transient ZFS Hamiltonian. It can be mainly attributed to the fluctuations of the static (in the molecular frame) ZFS Hamiltonian. As shown in Figure 7b,c, it implies similar drastic reductions of the integrands $g_2(t)G_{//}^{nor}$ and $g_2(t)$Re$[G_{\perp}^{nor}]$ of the spectral densities $j_{2//}(\omega_I)$ and $j_{2\perp}(\omega_S) \cong j_{2//}(\omega_I,B_0)$, which are quenched with respect to their ideal values. This yields the same relative important quenching of r_1^{OS} with respect to its ideal value displayed in the low-field range of Figure 6. This quenching can be used to determine the static ZFS Hamiltonian.

In the medium-field range, for example, $\nu_I = 20$ MHz, $G_{//}^{nor}$ has a quasi-monoexponential decay, very close to that of $G_{//T}^{nor} = \exp(-t/T_{1eT}^{McL})$ due to the sole transient ZFS Hamiltonian.[30] The decay of $G_{//}^{nor}$ is much slower at 20 MHz than at 1 MHz, so that the integrand $g_2(t)G_{//}^{nor}$ of $j_{2//}$ displayed in Figure 7b has much higher values at 20 MHz than at 1 MHz. Thus, the spectral density $j_{2//}$ is significantly larger at 20 MHz than at 1 MHz. In contrast, as shown in Figure 7a, Re$[G_{\perp}^{nor}]$ decays much faster than $G_{//}^{nor}$ and oscillates around 0 at the electronic Larmor frequency.[30] This decaying oscillatory behavior is transferred to the integrand $g_2(t)$Re$[G_{\perp}^{nor}]$ of $j_{2\perp}(\omega_S)$, which is shown in Figure 7c and averaged out to a small value of $j_{2\perp}(\omega_S)$ in the mathematical integration process. Thus, in the medium-field range, $j_{2\perp}(\omega_S) \ll j_{2//}(\omega_I,B_0)$ and $r_1^{OS} \cong Aj_{2//}$ gives information about the transient ZFS Hamiltonian that governs the increase of $j_{2//}$ and r_1^{OS} with field observed in Figure 6.

In the high-field range, for example, $\nu_I = 800$ MHz, $G_{//}^{nor}$ and $G_{//T}^{nor}$ have very slow superimposed decays.[30] The integrand $g_2(t)G_{//}^{nor}$ of $j_{2//}$ is no longer affected by $G_{//}^{nor} \cong 1$, so that $j_{2//}(\omega_I)$ takes its ideal expression $j_2(\omega_I)$ given by the cosine Fourier

transform in eq 4. Besides, the oscillations at the frequency ω_S of Re[$G_{\perp}^{nor}$], and therefore of the integrand $g_2(t)$Re [$G_{\perp}^{nor}$] displayed in Figure 7c, become so rapid[30] that $j_{2\perp}(\omega_S)$ vanishes. The relaxivity $r_1^{OS}(\omega_I)$ reduces to the star relaxivity $r_*^{OS}(\omega_I)$. Consequently, the value of r_1^{OS} measured at a given high field is simply r_*^{OS}, that is, apart form a multiplicative known factor, the value of the cosine Fourier transform of the DTCF $g_2(t)$ at the nuclear frequency ω_I in this field.

To sum up, the analysis of the experimental OS relaxivity r_1^{OS} at high, low, and medium-field values successively gives information on the DTCF $g_2(t)$, static ZFS Hamiltonian, and transient ZFS Hamiltonian. After determining $g_2(t)$ by the high-field procedure explained previously,[42] the relaxivity data at low or medium field are sufficiently numerous to characterize the ZFS Hamiltonian provided that it can be described by a reasonably small number of molecular parameters.

6. Water Proton Nuclear Magnetic Relaxation Dispersion

6.1. Water Outer-Sphere Dynamics and Star Relaxivity. The various OS relaxivities of the water protons can be calculated from its dipolar OS-DTCF $g_{2w}(t)$ with the help of eqs 5, 9, and 12. As shown in the Supporting Information Section II and Appendix B, the magnitude and time evolution of the OS-DTCF of a nuclear spin I on a molecule X are governed by the effective collision diameter $b_{eff,X}$ of X with Gd^{3+} given by eq II.2 and related with the OS collision surface of X with GdPA. Note that this surface is obtained as the set of the minimal distances between the center of X and Gd^{3+} corresponding to some collision criterion of X with GdPA. The small size of X with respect to GdPA and its fast tumbling justifies the replacement of the actual position of I by the center of X. The magnitude of the OS-DTCF scales with $b_{eff,X}^{-3}$ while its time argument scales with the effective translational correlation time $\tau_{eff,X} \equiv b_{eff,X}^2/D_X$ of X and GdL. Thus, according to Supporting Information eq II.3, the OS-DTCF for water can be calculated from the OS-DTCF for p-dioxane as

$$g_{2w}(t) = \left(\frac{b_{eff,dioxane}}{b_{eff,w}}\right)^3 g_{2dioxane}\left(t\frac{\tau_{eff,dioxane}}{\tau_{eff,w}}\right) \qquad (14)$$

In eq 14, the effective collision diameters $b_{eff,dioxane} = 5.63$ Å and $b_{eff,w} = 4.29$ Å, which are mean minimal effective Gd−H distances, were obtained by applying Supporting Information eq II.2 to the OS collision surfaces of p-dioxane and water shown in Figure 2. The correlation times $\tau_{eff,dioxane} = 273$ ps and $\tau_{eff,w} = 87$ ps are the ratios of the squares of the previous effective distances divided by the relative diffusion coefficients $D_{dioxane}$ and D_w of Supporting Information Table S1. The star relaxivities derived from the experimental OS-DTCFs of p-dioxane and water together with the limitations of the ABHF model are discussed in Supporting Information IV.2.

6.2. Relaxivity Mechanisms. Turn to the molecular interpretation of the measured relaxivities r_α^{exp} of the water protons. In particular, using the water proton OS relaxivity and the fluctuating ZFS Hamiltonian just determined, we will interpret the full longitudinal relaxivity profile of the water protons displayed in Figure 8 and assess the importance of the 2S relaxivity mechanism.

We begin with the high-field analysis, which is simpler since the relaxivites are independent of the ZFS Hamiltonian and the orientations of the $\overrightarrow{GdH}$ vectors of the H atoms of the IS and 2S water molecules. At 200, 400, 500 MHz, the OS relaxivities derived from the experimental OS-DTCF $g_{2w}(t)$ in eq 14 are

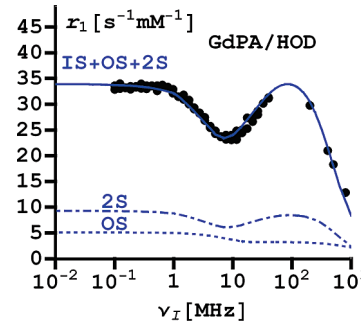

Figure 8. Longitudinal relaxivity profiles of the HOD protons I due to GdPA in D_2O at 298 K. The curves labeled OS and 2S are the purely OS and 2S contributions r_1^{OS} and r_1^{2S} to the total relaxivity r_1 given by eq 1, incorporating the IS contribution r_1^{IS}, and labeled IS + OS + 2S.

3.09, 2.84, 2.70 for r_1^{OS} and 3.84, 3.72, 3.65 for r_2^{OS}, respectively. They are about 50% larger than reasonable upper bounds of the ABHF predictions,[39] but still 7 to 10 times smaller than the measured relaxiviy r_α^{exp} displayed in Figures 8 and 9. Thus, the IS and/or 2S contributions are still strongly dominant even if the present corrected OS values are used. The drop of r_1^{exp} between 200 and 800 MHz is mainly caused by the decrease of the IS relaxivity r_1^{IS} in eq 6, which is driven by the $\omega_I^2\tau_r^2$ dispersion of $1/T_{1M}^{high\text{-}field}$ in eq 7 and by the decrease of the 2S relaxivity r_1^{2S} in eq A1, which is driven by the $\omega_I^2\tau_c'^2$ dispersion of $1/T'^{high\text{-}field}_{1M}$ in eq A2 of Supporting Information Appendix A. The measured r_1^{exp} drop implies that the rotational correlation time has to be fixed to the previously estimated value[39] $\tau_r = 386$ ps. Besides, the relative variations of $r_1^{exp} - r_1^{OS}$ and $r_2^{exp} - r_2^{OS}$ with field at high field mimic those of $1/T_{1M}^{high\text{-}field}$ and $1/T_{2M}^{high\text{-}field}$. This indicates that the coordination lifetime τ_M in eq 6 has no significant effect on the relaxivities. Then, it should be much shorter than $T_{1M}^{high\text{-}field}$ and $T_{2M}^{high\text{-}field}$, which are of the order of 1 μs at high field. This justifies the hypothesis $\tau_M \leq 100$ ns. Note that any choice of τ_M in this range leads to similar values of the IS relaxivities provided that $\tau_M \gg \tau_r$, so that the precise choice of τ_M is not relevant for the present interpretation. We somewhat arbitrarily chose the short value $\tau_M = 20$ ns that is consistent with the open coordination structure of PA. The confirmation of the IS parameters $q = 2$, $r_H = 3.1$ Å, $\tau_r = 386$ ps, $\tau_M = 20$ ns previously reported[39] is the first result of the high-field analysis just done. The high-field IS relaxivities calculated for these parameters are displayed in Figure 8 and 9. A second result is the evidence of large experimental 2S relaxivities $r_\alpha^{2S} \equiv r_\alpha^{exp} - r_\alpha^{OS} - r_\alpha^{IS}$. When B_0 raises from 200 to 500 MHz, r_1^{2S} decreases from 7.1 to 5.6 s^{-1} mM^{-1} and r_2^{2S} keeps a nearly constant value $\cong$ 11 s^{-1} mM^{-1}. Note that the experimental uncertainty ±15 ps on τ_r leads to variations of r_1^{IS} and r_2^{IS} less than 2.5 and 3.5%, respectively, and to subsequent changes of r_α^{2S} of the order of 5%, which confirm the necessity of strong 2S contributions to explain the experimental data.

The reliable molecular interpretation of the 2S relaxivities is an open question. Indeed, there are no experimental techniques available to measure the 2S parameters independently. Moreover, accurate ab initio simulations of the hydration dynamics of Ln^{3+} complexes are still limited to rather small ligands and durations of the order of a few tens of picoseconds.[68] They can hardly contribute to our understanding of the 2S dynamics with significantly longer characteristic times, especially in the case of a large complex like GdPA. Here, we propose an elementary, but coherent interpretation of the 2S mechanism based on classical molecular dynamics (MD) and qualitative physicochemical analysis. It is well established that the accurate

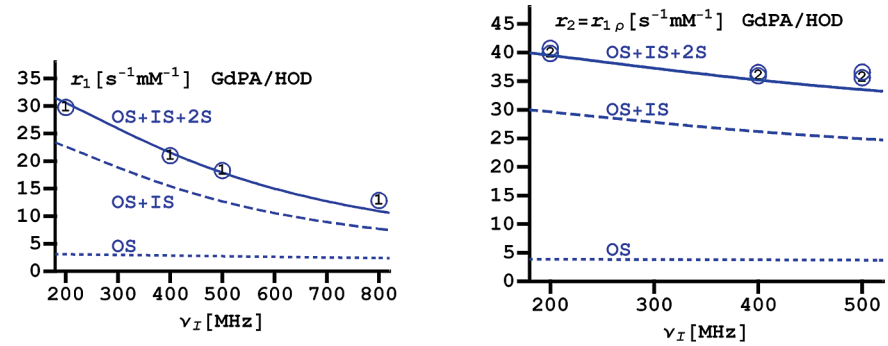

Figure 9. High-field dependence of the experimental and calculated relaxivities r_1 and $r_2 = r_{1\rho}$ of the HOD water (w) protons I due to GdPA in D_2O at 298 K. The OS contributions were obtained from the DTCF of the HOD proton in Figure 5. The IS contributions were calculated with $q = 2$, $r_H = 3.1$ Å, $\tau_r = 386$ ps, $\tau_M = 20$ ns. The 2S contributions were obtained with $q' = 3$, $r'_H = 3.68$ Å, $\tau'_M = 900$ ps. The curves labeled OS and OS+IS are the contributions r_α^{OS} and $r_\alpha^{OS} + r_\alpha^{IS}$ to the total relaxivities $r_\alpha = r_\alpha^{OS} + r_\alpha^{IS} + r_\alpha^{2S}$ labeled OS+IS+2S.

simulation of diffusion[69] and exchange processes[70] is a difficult task, the reliability of which requires very precise force fields including molecular polarizability.[55] In contrast, liquid structure is primarily governed by the excluded volume effects and the main electric interactions between unpolarizable molecules. It is also expected that the characteristic times of dynamic processes such as diffusion and 2S exchange through H-bond reorganization scale with the approximation of the electric intermolecular potentials. Thus, using the CHARMM software[59] with the simple TIP3 model[71] of water, the hydration structure and dynamics of GdPA was modeled by simulating the behavior of 843 water molecules around a single complex in a cubic simulation box of 30 Å side length. The computed pair distribution functions[72] of the water oxygen O and hydrogen H with respect to Gd^{3+} are displayed in Figure 3. The first peaks in the range [1.95 Å, 2.85 Å] for O and [2.35 Å, 3.25 Å] for H result from the $q = 2$ coordinated water molecules and their areas are 2 and 4, respectively. The second peaks are in the range [2.85 Å, 5.45 Å] for O and [3.25 Å, 4.25 Å] for H. They show the hydration structure around Gd^{3+}. They stem from the water molecules that do not coordinate Gd^{3+} but are close to this ion so that the relaxation rates of their protons can be strongly enhanced. These molecules are possible candidates to the 2S classification. In particular, the area of the H second peak is 6 and corresponds to 3 = 6/2 water molecules with favorably short Gd−H distances. This implies that the number q' of 2S water molecules should be limited to about 3.

Turn to the diffusion and 2S exchange dynamics of water. The used force field leads to a self-diffusion coefficient of water which is about three times the experimental value. To estimate the residence time of 2S water, the trajectories of the water molecules, the oxygen atoms of which enter the range of distances of the second peak, were followed during the 10 ns simulation. About 30 molecules remained for more than 100 ps in the second peak range and three of them stayed as long as 400 to 500 ps in this range. The actual residence times are expected to be three times longer in order to scale with the simulated diffusion that is about three times faster than in reality. Thus, the average residence time τ'_M can be as long as 1 to 2 ns. An excellent fit of the 2S relaxivity values $r_\alpha^{2S,exp} \equiv r_\alpha^{exp} - r_\alpha^{OS} - r_\alpha^{IS}$ by their theoretical counterparts in eqs A1 to A3 is obtained with the 2S parameters $q' = 3$, $r'_H = 3.68$ Å, $\tau'_M = 900$ ps, which are compatible with the simulation results. Though rather long,[36,73] τ'_M has a value similar to that encountered with a 1,4,7,10-tetraazacyclododecane containing a carboxamide substituent[35] or human serum albumin.[37] The total theoretical relaxivities $r_\alpha^{th} = r_\alpha^{OS} + r_\alpha^{IS} + r_\alpha^{2S}$ displayed at high field in Figures 8 and 9 compare very well with the experimental relaxivities. Moreover, using the ZFS Hamiltonian parameters derived previously, the theoretical relaxivity profile can be computed with the help of the Grenoble method. Assume that the $\overrightarrow{GdH}$ vectors of IS and 2S water in the molecular frame (P_S) of the principal axes of the static ZFS Hamiltonian have isotropic random orientations in this frame. Assume that the orientation weights entering the expressions of the IS and 2S relaxivities given by eqs 6 and 11 and A1, A4, and A5 are $w_{\hat{x}_S} = w_{\hat{y}_S} = w_{\hat{z}_S} = 1/3$ and $w'_{\hat{x}_S} = w'_{\hat{y}_S} = w'_{\hat{z}_S} = 1/3$. The values of r_1^{th} are in very good agreement with their experimental counterparts. They are just 5% too large in the low-field range. Remember that the information on the water OS dynamics and ZFS Hamiltonian was derived from an auxiliary OS probe. The fact that this independent information combined with a high-field analysis of the water proton relaxivities provided us with the necessary parameters to compute a theoretical relaxivity profile in very good agreement with experiment should be emphasized. Besides, if the orientation weights of the IS contribution have the slightly modified values $w_{\hat{x}_S} = w_{\hat{y}_S} = 0.38$, $w_{\hat{z}_S} = 0.24$, which indicates a tendency of the $\overrightarrow{GdH}$ vectors to be in the equatorial plane of (P_S), the total theoretical relaxivity r_1^{th} displayed in Figure 8 agrees perfectly with experiment over the whole frequency range.

To be complete, note that the systematic, but very small relaxivity enhancements stemming from the Curie "spin" relaxation[5] due to Gd^{3+} were taken into account to interpret the measured values with the help of eq C8 of Supporting Information Appendix C.

7. Conclusion

Because of their influence on the contrast efficiency of many Gd^{3+} complexes, the electronic spin relaxation, the OS contribution, and the 2S contribution should be properly evaluated and interpreted. For that purpose, we have resorted to a purely OS probe, the DTCF $g_{2probe}(t)$ of which can be easily derived from experiment.

The determination of the experimental OS-DTCF $g_{2probe}(t)$ of a probe solute is of general scope for a complex GdL and more generally for paramagnetic species with slow electronic spin relaxation at high field.[42] The usefulness of this property, just shown for relaxation contrast agents, should concern other major issues such as the identification of protein surfaces for drug design,[74,75] the auxiliary OS investigation of the compactness of protein domains by suitable placement of the paramagnetic center,[76] the demanding validation of force fields,[42,77] the evaluation of solvation effects on ion−ion interactions,[65,66,78] or the development of responsive PARACEST agents.[79] There-

fore, the method for determining $g_{2probe}(t)$ is summarized now. Let τ be the correlation time of the relative translational motion of the probe solute with respect to GdL. By suitable T_1 and T_2 (or $T_{1\rho}$) measurements, the star relaxivity r_*^{OS} associated with $g_{2probe}(t)$ is measured at zero frequency and over the largest possible range of high frequency values loosely defined by $\omega_I\tau \geq 1$, where ω_I is the proton angular Larmor frequency. Using a field/temperature correspondence between the values of the OS relaxivity r_*^{OS}, the upper-bound of the high-frequency range can be increased by lowering the temperature of the solution in order to determine this relaxivity over a frequency domain of sufficient extension. Then, combining the measured values of r_*^{OS} with model-free properties of $g_{2probe}(t)$ and r_*^{OS}, both functions can be derived simultaneously. For the method to work, $g_{2probe}(t)$ should display the universal long-time decay in $(Dt)^{-3/2}$, where D is the measured diffusion coefficient of the probe solute and GdL. This happens in the absence of long-ranged Coulomb interaction between these species, so that the method applies either if at least one of them is neutral or if both are charged in a solution of sufficiently high ionic strength like normal saline.

We have used the probe solute method for deciphering the water (proton) relaxivity mechanisms of a cyclodecapeptide complex GdPA at concentrations lower than 1 mM. We have determined the dipolar OS-DTCF $g_{2probe}(t)$ of the probe solute p-dioxane. As a first application, we have characterized the fluctuating ZFS Hamiltonian responsible for the electronic relaxation of the Gd^{3+} spin. Indeed, the measured longitudinal relaxivity of the dioxane protons is quenched by the electronic spin relaxation at low and medium field. At low field, the electronic spin relaxation is dominated by the fluctuations of the "static" (in the molecular frame) ZFS Hamiltonian due to the Brownian rotation of the complex in the laboratory frame. The relaxivity quenching allowed us to measure the amplitude of the static ZFS Hamiltonian and again confirm the previously derived value $\tau_r = 386$ ps of the rotational correlation time of GdPA. At medium field, the electronic spin relaxation depends mainly on the fluctuations of the transient ZFS Hamiltonian caused by the intramolecular atomic motions (distorsions and vibrations) of the PA ligand. From the relaxivity quenching of the dioxane protons we obtained the amplitude Δ_T and "vibrational" correlation time $\tau_v = 9$ ps of the transient ZFS Hamiltonian. As shown in Supporting Information IV.1, this rather long τ_v accounts for the collective displacements of the atoms of the flexible PA ligand corresponding to low-frequency vibrational modes[80,81] and justifies the theoretical efforts toward a more elaborate description of the transient ZFS Hamiltonian.[82−84]

Then, we have derived the OS-DTCF $g_{2w}(t)$ for water from its counterpart $g_{2dioxane}(t)$ for dioxane by scaling according to the simulated collision geometry and relative diffusion coefficient of these molecules with respect to GdPA. At high field, using the accurate water IS relaxivities r_α^{IS} from a previous analysis[39] and the water OS relaxivities r_α^{OS} calculated from $g_{2w}(t)$, we have obtained large 2S relaxivity residuals $r_\alpha^{2S} \equiv r_\alpha^{exp} - r_\alpha^{OS} - r_\alpha^{IS}$, confirming the existence of a strong 2S mechanism unambiguously.

On the whole, the present relaxivity analysis, which rests on general, simple, and safe hypotheses without overinterpretation of the data, is justified by the excellent agreement between experiment and theory over a very large frequency range for both the p-dioxane and HOD protons.

Acknowledgment. We thank P.-A. Bayle and A. Favier for their help to use the CGRM and IBS NMR facilities. We are indebted to Dr. M. Defranceschi and the CEA/DEN for the purchase of the Stelar relaxometer. This work is a contribution to the EC COST Action D-38 and European EMIL network.

Supporting Information Available: Experimental data (self-diffusion coefficients, NMR relaxation), simulation details, relaxivity theory (mathematical details), peripheral findings (rationale of the ZFS Hamiltonian parameters, limitations of the ABHF outer-sphere model), and complete ref 16. This material is available free of charge via the Internet at http://pubs.acs.org.

References and Notes

(1) Abragam, A.; Bleaney, B. *Résonance Paramagnétique Electronique des Ions de Transition*; Presses Universitaires de France: Paris, 1971.
(2) Canet, D. *Adv. Inorg. Chem.* **2005**, *57*, 3–40.
(3) Kowalewski, J.; Nordenskiold, L.; Benetis, N.; Westlund, P. O. *Prog. Nucl. Magn. Reson. Spectrosc.* **1985**, *17*, 141–185.
(4) Peters, J. A.; Huskens, J.; Raber, D. J. *Prog. Nucl. Magn. Reson. Spectrosc.* **1996**, *28*, 283–350.
(5) Bertini, I.; Luchinat, C.; Parigi, G. *Solution NMR of Paramagnetic Molecules*; Elsevier: Amsterdam, 2001.
(6) Kowalewski, J.; Kruk, D.; Parigi, G. *Adv. Inorg. Chem.* **2005**, *57*, 41–104.
(7) Helm, L. *Prog. Nucl. Magn. Reson. Spectrosc.* **2006**, *49*, 45–64.
(8) Caravan, P.; Ellison, J. J.; McMurry, T. J.; Lauffer, R. B. *Chem. Rev.* **1999**, *99*, 2293–2352.
(9) *The Chemistry of Contrast Agents*; Merbach, A. E., Toth, E., Eds.; Wiley: New York, 2001.
(10) Aime, S.; Botta, M.; Terreno, E. *Adv. Inorg. Chem.* **2005**, *57*, 173–237.
(11) Caravan, P. *Chem. Soc. Rev.* **2006**, *35*, 512–523.
(12) Aime, S.; Castelli, D. D.; Crich, S. G.; Gianolio, E.; Terreno, E. *Acc. Chem. Res.* **2009**, *42*, 822–831.
(13) De Leon-Rodriguez, L. M.; Lubag, A. J. M.; Malloy, C. R.; Martinez, G. V.; Gillies, R. J.; Sherry, A. D. *Acc. Chem. Res.* **2009**, *42*, 948–957.
(14) Caravan, P. *Acc. Chem. Res.* **2009**, *42*, 851–862.
(15) Major, J. L.; Meade, T. J. *Acc. Chem. Res.* **2009**, *42*, 893–903.
(16) Yang, J. J.; et al. *J. Am. Chem. Soc.* **2008**, *130*, 9260–9267.
(17) Belorizky, E.; Fries, P. H.; Helm, L.; Kowalewski, J.; Kruk, D.; Sharp, R. R.; Westlund, P.-O. *J. Chem. Phys.* **2008**, *128*, 052315.
(18) Aman, K.; Westlund, P. O. *Phys. Chem. Chem. Phys.* **2007**, *9*, 691–700.
(19) Bonnet, C. S.; Fries, P. H.; Gadelle, A.; Gambarelli, S.; Delangle, P. *J. Am. Chem. Soc.* **2008**, *130*, 10401–10413.
(20) Lauffer, R. B. *Chem. Rev.* **1987**, *87*, 901–927.
(21) Woessner, D. E. *J. Chem. Phys.* **1962**, *37*, 647–654.
(22) Abragam, A. *Les Principes du Magnétisme Nucléaire*; Presses Universitaires de France: Paris, 1961.
(23) Powell, D. H.; NiDhubhghaill, O. M.; Pubanz, D.; Helm, L.; Lebedev, Y. S.; Schlaepfer, W.; Merbach, A. E. *J. Am. Chem. Soc.* **1996**, *118*, 9333–9346.
(24) Borel, A.; Toth, E.; Helm, L.; Janossy, A.; Merbach, A. E. *Phys. Chem. Chem. Phys.* **2000**, *2*, 1311–1317.
(25) Rast, S.; Fries, P. H.; Belorizky, E. *J. Chim. Phys. Phys.-Chim. Biol.* **1999**, *96*, 1543–1550.
(26) Rast, S.; Fries, P. H.; Belorizky, E. *J. Chem. Phys.* **2000**, *113*, 8724–8735.
(27) Rast, S.; Borel, A.; Helm, L.; Belorizky, E.; Fries, P. H.; Merbach, A. E. *J. Am. Chem. Soc.* **2001**, *123*, 2637–2644.
(28) Belorizky, E.; Fries, P. H. *Phys. Chem. Chem. Phys.* **2004**, *6*, 2341–2351.
(29) Fries, P. H.; Belorizky, E. *J. Chem. Phys.* **2005**, *123*, 124510.
(30) Fries, P. H.; Belorizky, E. *J. Chem. Phys.* **2007**, *126*, 204503.
(31) Werner, E. J.; Avedano, S.; Botta, M.; Hay, B. P.; Moore, E. G.; Aime, S.; Raymond, K. N. *J. Am. Chem. Soc.* **2007**, *129*, 1870–1871.
(32) Borel, A.; Bean, J. F.; Clarkson, R. B.; Helm, L.; Moriggi, L.; Sherry, A. D.; Woods, M. *Chem. Eur. J.* **2008**, *14*, 2658–2667.
(33) Avedano, S.; Tei, L.; Lombardi, A.; Giovenzana, G. B.; Aime, S.; Longo, D.; Botta, M. *Chem. Commun.* **2007**, 4726–4728.
(34) Caravan, P.; Parigi, G.; Chasse, J. M.; Cloutier, N. J.; Ellison, J. J.; Lauffer, R. B.; Luchinat, C.; McDermid, S. A.; Spiller, M.; McMurry, T. J. *Inorg. Chem.* **2007**, *46*, 6632–6639.
(35) Aime, S.; Botta, M.; Parker, D.; Williams, J. A. G. *J. Chem. Soc., Dalton Trans.* **1996**, 17–23.
(36) Botta, M. *Eur. J. Inorg. Chem.* **2000**, 399–407.
(37) Caravan, P.; Cloutier, N. J.; Greenfield, M. T.; McDermid, S. A.; Dunham, S. U.; Bulte, J. W. M.; Amedio, J. C.; Looby, R. J.; Supkowski,

R. M.; Horrocks, W. D.; McMurry, T. J.; Lauffer, R. B. *J. Am. Chem. Soc.* **2002**, *124*, 3152–3162.
(38) Vander Elst, L.; Port, M.; Raynal, I.; Simonot, C.; Muller, R. N. *Eur. J. Inorg. Chem.* **2003**, 2495–2501.
(39) Bonnet, C. S.; Fries, P. H.; Crouzy, S.; Seneque, O.; Cisnetti, F.; Boturyn, D.; Dumy, P.; Delangle, P. *Chem. Eur. J.* **2009**, *15*, 7083–7093.
(40) Ayant, Y.; Belorizky, E.; Alizon, J.; Gallice, J. *J. Phys. (Paris)* **1975**, *36*, 991–1004.
(41) Hwang, L. P.; Freed, J. H. *J. Chem. Phys.* **1975**, *63*, 4017–4025.
(42) Fries, P. H.; Imbert, D.; Melchior, A. *J. Chem. Phys.* **2010**, *132*, 044502.
(43) Borel, A.; Helm, L.; Merbach, A. E.; Atsarkin, V. A.; Demidov, V. V.; Odintsov, B. M.; Belford, R. L.; Clarkson, R. B. *J. Phys. Chem. A* **2002**, *106*, 6229–6231.
(44) Benmelouka, M.; Van Tol, J.; Borel, A.; Port, M.; Helm, L.; Brunel, L. C.; Merbach, A. E. *J. Am. Chem. Soc.* **2006**, *128*, 7807–7816.
(45) Fries, P. H.; Gateau, C.; Mazzanti, M. *J. Am. Chem. Soc.* **2005**, *127*, 15801–15814.
(46) Dunand, F. A.; Borel, A.; Merbach, A. E. *J. Am. Chem. Soc.* **2002**, *124*, 710–716.
(47) Kowalewski, J.; Mäler, L. *Nuclear Spin Relaxation in Liquids: Theory, Experiments, and Applications*; Taylor & Francis: London, 2006.
(48) Strandberg, E.; Westlund, P. O. *J. Magn. Reson., Ser. A* **1996**, *122*, 179–191.
(49) Zhou, X. Z.; Caravan, P.; Clarkson, R. B.; Westlund, P. O. *J. Magn. Reson.* **2004**, *167*, 147–160.
(50) Zhou, X. Z.; Westlund, P. O. *J. Magn. Reson.* **2005**, *173*, 75–83.
(51) Benmelouka, M.; Borel, A.; Moriggi, L.; Helm, L.; Merbach, A. E. *J. Phys. Chem. B* **2007**, *111*, 832–840.
(52) Westlund, P. O.; Larsson, T. P.; Teleman, O. *Mol. Phys.* **1993**, *78*, 1365–1384.
(53) Westlund, P. O. *Mol. Phys.* **1995**, *85*, 1165–1178.
(54) Fries, P. H. *J. Chem. Phys.* **2010**, *132*, 224103.
(55) Clavaguera, C.; Sansot, E.; Calvo, F.; Dognon, J. P. *J. Phys. Chem. B* **2006**, *110*, 12848–12851.
(56) Clavaguera, C.; Pollet, R.; Soudan, J. M.; Brenner, V.; Dognon, J. P. *J. Phys. Chem. B* **2005**, *109*, 7614–7616.
(57) Caravan, P.; Astashkin, A. V.; Raitsimring, A. M. *Inorg. Chem.* **2003**, *42*, 3972–3974.
(58) Helm, L.; Merbach, A. E. *Chem. Rev.* **2005**, *105*, 1923–1959.
(59) Brooks, B. R.; Bruccoleri, R. E.; Olafson, B. D.; States, D. J.; Swaminathan, S.; Karplus, M. *J. Comput. Chem.* **1983**, *4*, 187–217.
(60) Halle, B. *J. Chem. Phys.* **2003**, *119*, 12372–12385.
(61) Vigouroux, C.; Bardet, M.; Belorizky, E.; Fries, P. H.; Guillermo, A. *Chem. Phys. Lett.* **1998**, *286*, 93–100.
(62) Vigouroux, C.; Belorizky, E.; Fries, P. H. *Eur. Phys. J. D* **1999**, *5*, 243–255.
(63) Fries, P. H.; Ferrante, G.; Belorizky, E.; Rast, S. *J. Chem. Phys.* **2003**, *119*, 8636–8644.
(64) Nonat, A.; Fries, P. H.; Pecaut, J.; Mazzanti, M. *Chem. Eur. J.* **2007**, *13*, 8489–8506.
(65) Sacco, A.; Belorizky, E.; Jeannin, M.; Gorecki, W.; Fries, P. H. *J. Phys. II* **1997**, *7*, 1299–1322.
(66) Fries, P. H.; Richardi, J.; Rast, S.; Belorizky, E. *Pure Appl. Chem.* **2001**, *73*, 1689–1703.
(67) Rast, S.; Fries, P. H.; Belorizky, E.; Borel, A.; Helm, L.; Merbach, A. E. *J. Chem. Phys.* **2001**, *115*, 7554–7563.
(68) Pollet, R.; Marx, D. *J. Chem. Phys.* **2007**, *126*, 181102.
(69) Mahoney, M. W.; Jorgensen, W. L. *J. Chem. Phys.* **2001**, *114*, 363–366.
(70) Kowall, T.; Foglia, F.; Helm, L.; Merbach, A. E. *J. Am. Chem. Soc.* **1995**, *117*, 3790–3799.
(71) Jorgensen, W. L.; Chandrasekhar, J.; Madura, J. D.; Impey, R. W.; Klein, M. L. *J. Chem. Phys.* **1983**, *79*, 926–935.
(72) Hansen, J.-P.; McDonald, I. R. *Theory of Simple Liquids*, 3rd ed.; Academic Press: London, 2006.
(73) Bleuzen, A.; Foglia, F.; Furet, E.; Helm, L.; Merbach, A. E.; Weber, J. *J. Am. Chem. Soc.* **1996**, *118*, 12777–12787.
(74) Pintacuda, G.; Otting, G. *J. Am. Chem. Soc.* **2002**, *124*, 372–373.
(75) Bernini, A.; Venditti, V.; Spiga, O.; Niccolai, N. *Prog. Nucl. Magn. Reson. Spectrosc.* **2009**, *54*, 278–289.
(76) Xue, Y.; Podkorytov, I. S.; Rao, D. K.; Benjamin, N.; Sun, H. L.; Skrynnikov, N. R. *Protein Sci.* **2009**, *18*, 1401–1424.
(77) Trbovic, N.; Kim, B.; Friesner, R. A.; Palmer, A. G. *Proteins: Struct., Funct., Bioinf.* **2008**, *71*, 684–694.
(78) Canard, G.; Piguet, C. *Inorg. Chem.* **2007**, *46*, 3511–3522.
(79) Huang, C. H.; Morrow, J. R. *J. Am. Chem. Soc.* **2009**, *131*, 4206–4207.
(80) Swaminathan, S.; Ichiye, T.; Vangunsteren, W.; Karplus, M. *Biochemistry* **1982**, *21*, 5230–5241.
(81) Marco, E.; Gago, F. *ChemMedChem* **2007**, *2*, 1388–1401.
(82) Odelius, M.; Ribbing, C.; Kowalewski, J. *J. Chem. Phys.* **1995**, *103*, 1800–1811.
(83) Sharp, R.; Lohr, L. *J. Chem. Phys.* **2001**, *115*, 5005–5014.
(84) Lindgren, M.; Laaksonen, A.; Westlund, P. O. *Phys. Chem. Chem. Phys.* **2009**, *11*, 10368–10376.

JP101443V